


RESEARCH

Open Access



Imaging of $\alpha_v\beta_3$ integrin expression in experimental myocardial ischemia with [^{68}Ga]NODAGA-RGD positron emission tomography

Maria Grönman¹ , Miikka Tarkia¹, Tuomas Kiviniemi², Paavo Halonen³, Antti Kuivanen³, Timo Savunen^{2,4}, Tuula Tolvanen^{5,6}, Jarmo Teuho^{5,6}, Meeri Käkelä¹, Olli Metsälä¹, Mikko Pietilä², Pekka Saukko⁷, Seppo Ylä-Herttuala³, Juhani Knuuti^{1,5}, Anne Roivainen^{1,5,8} and Antti Saraste^{1,2,5,9*}

Abstract

Background: Radiolabeled RGD peptides detect $\alpha_v\beta_3$ integrin expression associated with angiogenesis and extracellular matrix remodeling after myocardial infarction. We studied whether cardiac positron emission tomography (PET) with [^{68}Ga]NODAGA-RGD detects increased $\alpha_v\beta_3$ integrin expression after induction of flow-limiting coronary stenosis in pigs, and whether $\alpha_v\beta_3$ integrin is expressed in viable ischemic or injured myocardium.

Methods: We studied 8 Finnish landrace pigs 13 \pm 4 days after percutaneous implantation of a bottleneck stent in the proximal left anterior descending coronary artery. Antithrombotic therapy was used to prevent stent occlusion. Myocardial uptake of [^{68}Ga]NODAGA-RGD (290 \pm 31 MBq) was evaluated by a 62 min dynamic PET scan. The ischemic area was defined as the regional perfusion abnormality during adenosine-induced stress by [^{15}O]water PET. Guided by triphenyltetrazolium chloride staining, tissue samples from viable and injured myocardial areas were obtained for autoradiography and histology.

Results: Stent implantation resulted in a partly reversible myocardial perfusion abnormality. Compared with remote myocardium, [^{68}Ga]NODAGA-RGD PET showed increased tracer uptake in the ischemic area (ischemic-to-remote ratio 1.3 \pm 0.20, $p = 0.0034$). Tissue samples from the injured areas, but not from the viable ischemic areas, showed higher [^{68}Ga]NODAGA-RGD uptake than the remote non-ischemic myocardium. Uptake of [^{68}Ga]NODAGA-RGD correlated with immunohistochemical detection of $\alpha_v\beta_3$ integrin that was expressed in the injured myocardial areas.

Conclusions: Cardiac [^{68}Ga]NODAGA-RGD PET demonstrates increased myocardial $\alpha_v\beta_3$ integrin expression after induction of flow-limiting coronary stenosis in pigs. Localization of [^{68}Ga]NODAGA-RGD uptake indicates that it reflects $\alpha_v\beta_3$ integrin expression associated with repair of recent myocardial injury.

Keywords: Positron emission tomography, Myocardial ischemia, Angiogenesis, $\alpha_v\beta_3$ integrin

Background

Integrins are heterodimeric transmembrane glycoprotein receptors that mediate interactions between cells and their surroundings [1, 2]. Imaging of radiolabelled arginyl-glycyl-aspartic acid (RGD) motif containing peptides targeting the $\alpha_v\beta_3$ integrin has demonstrated enhanced myocardial $\alpha_v\beta_3$ integrin expression after

ischemic myocardial injury [3–15]. The $\alpha_v\beta_3$ integrin is expressed in cardiac myofibroblasts [10, 16] and macrophages [17] involved in extracellular matrix (ECM) remodeling as well as in vascular endothelial cells during angiogenesis [3–9, 11, 13, 18], i.e. the formation of new microvascular networks from pre-existing capillaries. Since ECM remodeling and angiogenesis are essential for the healing of ischemic injury $\alpha_v\beta_3$ integrin expression has been proposed as a marker of myocardial repair [3, 18]. However, it remains unknown to what extent the $\alpha_v\beta_3$ integrin is expressed in response to chronic

*Correspondence: antsaras@utu.fi

¹ Turku PET Centre, University of Turku, 20521 Turku, Finland
Full list of author information is available at the end of the article

flow-limiting coronary stenosis and whether $\alpha_v\beta_3$ integrin expression is induced in viable or irreversibly injured myocardium. We hypothesized that in addition to the injured myocardium ischemia induces angiogenesis and $\alpha_v\beta_3$ integrin expression also in the viable ischemic myocardium.

In order to study the effects of flow-limiting coronary stenosis on myocardial expression of $\alpha_v\beta_3$ integrin, we performed cardiac positron emission tomography (PET) with ^{68}Ga -labeled 1,4,7-triazacyclononane-1-glutaric acid-4,7-diacetic acid conjugated RGD peptide (^{68}Ga]NODAGA-RGD), a myocardial perfusion PET, and a histological evaluation of myocardial injury and $\alpha_v\beta_3$ integrin expression in pigs. We induced stenosis by percutaneous implantation of a bottleneck stent in the proximal left anterior descending (LAD) coronary artery that has been shown to induce severe reduction in myocardial perfusion, rapid collateral formation and some degree of irreversible myocardial injury [19]. We compared ^{68}Ga]NODAGA-RGD uptake in the ischemic myocardium and the remote non-ischemic myocardium as well as in the viable and injured ischemic myocardial areas 2 weeks after the induction of stenosis.

Methods

Animals and study protocol

Coronary stenosis was created in 11 domestic, 3-month old pigs weighing 30–35 kg by implanting a bottleneck stent in the proximal LAD coronary artery as described previously [19]. In addition, a sham group of 4 pigs underwent a catheterization procedure without the stent implantation. Myocardial ^{68}Ga]NODAGA-RGD uptake was evaluated by PET 13 \pm 4 days after the stent implantation. In the same imaging session, myocardial perfusion was quantified using ^{15}O]water PET (physical half-life 2 min) at rest and during adenosine-induced stress before a ^{68}Ga]NODAGA-RGD (physical half-life 68 min) injection to localize the myocardium and to determine the ischemic area. Three pigs without a perfusion defect during adenosine stress were considered as procedural failures and excluded from further in vivo analyses.

Subsequently, the pigs were euthanized and their hearts were excised. Based on 1% 2,3,5-triphenyltetrazolium chloride (TTC) (Sigma-Aldrich, Saint Louis, MO, USA) staining, tissue samples were obtained from the injured ischemic (TTC negative) and adjacent viable ischemic (TTC positive) myocardium as well as from the remote non-ischemic myocardium. Autoradiography of myocardial tissue sections was used to compare ^{68}Ga]NODAGA-RGD uptake with the histology, $\alpha_v\beta_3$ integrin expression and CD31 on endothelial cells.

Anesthesia and hemodynamic monitoring

Prior to the cardiac catheterization and imaging studies, the animals were anesthetized with midazolam 1 mg/kg (Midazolam Hameln, Hameln Pharmaceuticals GmbH, Hameln, Germany) and xylazine 4 mg/kg (Rompun vet, Bayer Animal Health GmbH, Leverkusen, Germany) intramuscularly (i.m), connected to a respirator (Dräger Oxylog 3000, Drägerwerk AG, Lübeck, Germany) and ventilated mechanically (tidal volume 8–10 ml/kg, frequency 14–18 breaths per minute). The ear vein was cannulated using a 22G venous catheter and anesthesia was maintained with intravenous (i.v.) infusion of propofol 10–50 mg/kg/h (Propofol-Lipuro, B. Braun Melsungen AG, Melsungen, Germany) combined with fentanyl 4–8 $\mu\text{g}/\text{kg}/\text{h}$ (Fentanyl-Hameln, Hameln Pharmaceuticals GmbH, Hameln, Germany). Cefuroxime (Zinacef, Glaxo-SmithKline, Brentford, UK) was given 750 mg i.v. before catheterization.

The femoral artery was cannulated for hemodynamic monitoring during imaging studies. Diastolic, systolic and mean arterial pressure and heart rate were recorded using a pressure transducer (TruWave, Edwards Lifesciences, Irvine, CA, USA) connected to an anesthesia monitor.

Coronary stenosis model

The bottleneck stent was prepared and implanted as previously described [19]. In brief, an introducer sheath (6F, Cordis, Bridgewater, NJ, USA) was placed percutaneously in the femoral artery. Catheterization of the pigs was performed in an angiographic laboratory equipped with a GE Innova 3100^{IQ} three-dimensional (3-D) angiography device (GE Healthcare, Waukesha, WI, USA). To create a coronary stenosis, a sterilized polytetrafluoroethylene tube (diameter 5/64 in.; Fluorplast, Petalax, Finland) with a bottleneck diameter of 0.9 mm was inserted on a Coroflex Blue Ultra (B. Braun Medical; profile 0.8 mm) bare metal stent. The bottleneck stent was placed into the proximal LAD. The correct positioning and patency of the bottleneck stent was confirmed by X-ray fluoroscopy, the sheath was removed and the Femostop device (St. Jude Medical, St. Paul, MN, USA) was used to secure hemostasis.

To prevent ischemia-induced arrhythmias, administration of amiodarone 200 mg/day per orally (p.o.) (Cordarone, Sanofi, Paris, France) and bisoprolol 2.5 mg/day p.o. (Bisoproact, Actavis Group, Hafnarfjörður, Iceland) were administered starting 1 week before the procedure until the end of the study. Immediately before stent implantation, the pigs also received a 100 mg i.v. bolus of lidocaine (Lidocain, Orion Corporation, Espoo, Finland) and 2.5 ml i.v. bolus of magnesium sulphate (246 mg/ml, Addex-magnesiumsulfaatti, Fresenius Kabi AB, Uppsala,

Sweden). To prevent thrombotic occlusion of the bottleneck stent, acetylsalicylic acid 300 mg p.o. (Primaspan, Orion Corporation, Espoo, Finland) and clopidogrel 300 mg p.o. (Plavix, Sanofi, Paris, France) were given 1 day before stenting. Furthermore, enoxaparin 30 mg i.v. (Sanofi, Paris, France) was administered after the insertion of an introducer sheath in the femoral artery, and another 30 mg was given subcutaneously (s.c.) after removing the sheath and securing hemostasis. Daily doses of acetylsalicylic acid (100 mg/day p.o.), clopidogrel (75 mg/day p.o.), and enoxaparin (30 mg/day s.c.) were continued throughout the study.

Radiochemistry

1,4,7-Triazacyclononane-1-glutaric acid-4,7-diacetic acid conjugated RGD peptide (cyclo[L-arginylglycyl-L-aspartyl-D-tyrosyl-N6-([[4,7-bis(carboxymethyl)-1,4,7-triazonan-1-yl]acetyl)]-L-lysyl]; NODAGA-RGD) was purchased from ABX advanced biochemical compounds GmbH (product number 9805; Radenberg, Germany). ^{68}Ga was obtained from a $^{68}\text{Ge}/^{68}\text{Ga}$ generator (Eckert & Ziegler, Valencia, CA, USA) by elution with 0.1 M hydrochloric acid. ^{68}Ga -eluate (500 μl) was mixed with sodium acetate (18 mg) to give a pH of approximately 5. Then, NODAGA-RGD (10 nmol, dissolved in deionized water to give stock solution of 1 mM) was added. The reaction mixture was heated at 100 °C for 15 min. No further purification was performed. The radiochemical purity of ^{68}Ga NODAGA-RGD was determined by reversed-phase high-performance liquid chromatography (RP-HPLC) with a Jupiter C18 column (4.6 \times 150 mm, 300 Å, 5 μm ; Phenomenex, Torrance, CA, USA). The HPLC conditions were as follows: flow rate = 1 ml/min, λ = 220 nm. The gradient system was: A = 0.1% trifluoroacetic acid (TFA) in water; B = 0.1% TFA in acetonitrile. The A/B gradient was: 0–5 min 97/3, 5–15 min from 97/3 to 0/100. The HPLC system consisted of LaChrom Instruments (Hitachi; Merck, Darmstadt, Germany) coupled with a flow-through Radiomatic 150TR radioisotope detector (Packard, Meriden, CT, USA).

In vitro plasma protein binding

To evaluate species-dependent differences, the ^{68}Ga NODAGA-RGD binding to human, pig and rat plasma proteins was measured using in vitro assay as described previously [20].

PET image acquisition and reconstruction

All the animals first underwent a myocardial perfusion PET study with ^{15}O water at rest and under pharmacological stress as previously described [21] with a Discovery 690 hybrid PET/CT scanner (GE Medical Systems, Milwaukee, WI, USA). ^{15}O water (760 \pm 130 MBq) was

injected as an i.v. bolus over 15 s at an infusion rate of 10 ml/min via the ear vein. A dynamic acquisition of 4 min 40 s was performed (time frames 14 \times 5 s, 3 \times 10 s, 3 \times 20 s and 4 \times 30 s) in 3D mode. An adenosine infusion at the rate of 200–500 $\mu\text{g}/\text{kg}/\text{min}$ combined with phenylephrine 5 $\mu\text{g}/\text{kg}/\text{min}$ was started 120 s before the ^{15}O water injection and continued until the end of the scan. The acquired ^{15}O water PET data were corrected for scatter, random counts and dead time, and reconstructed with an iterative VUE Point algorithm using 2 iterations and 24 subsets. The device produces 47 axial planes with a slice thickness of 3.27 mm.

Then a ^{68}Ga NODAGA-RGD PET was performed with an ECAT EXACT HR+ scanner (Siemens-CTI, Knoxville, TN, USA). The studies were started with a 10 min transmission scan. The dynamic scanning started at the same time as 310 \pm 43 MBq (230–400 MBq) of ^{68}Ga NODAGA-RGD was injected via the ear vein. The acquisition time frames were as follows: 18 \times 10 s, 4 \times 30 s, 2 \times 120 s, 1 \times 180 s, 4 \times 300 s, 3 \times 600 s (total duration 62 min). The acquired ^{68}Ga NODAGA-RGD PET data were corrected for scatter, random counts, and dead time and iteratively reconstructed with ordered-subsets expectation maximization (OSEM) algorithm using 2 iterations and 32 subsets. The whole transaxial field of view (70 cm) was reconstructed in 256 \times 256 matrix yielding to pixel size of 2.57 mm \times 2.57 mm. The device produces 63 axial planes with a slice thickness of 2.43 mm.

PET image analysis

PET image analysis was done with Carimas 2.9 software (Turku PET Centre, Turku, Finland) using Heart and Polar-Roi plug-in tools as described earlier [21, 22]. After manual definition of the long axis, the myocardial contours in the ^{15}O water images were semi-automatically defined. In order to obtain myocardial time-activity curves (TAC; the radioactivity concentrations as a function of time after the tracer injection), the PET data were volumetrically sampled and the volume of interest (VOI) covering the whole left ventricle (LV) myocardium was applied to the dynamic imaging series. The arterial input function was measured in a VOI centered in the basal part of the LV cavity. The regional LV myocardial blood flow (MBF) was quantified in ^{15}O water data as ml/min/g using a conventional single-compartment model and displayed as a parametric polar map with a standard 17 segments. The polar maps were normalized to one segment (segment 11) in the posterolateral wall that was always outside the ischemic area. The ischemic area was defined as a region with myocardial blood flow less than 80% of maximum during adenosine-induced stress as previously described [22].

For quantification of ^{68}Ga NODAGA-RGD uptake in the myocardium, the ^{15}O water images and the ^{68}Ga

NODAGA-RGD images were co-registered using the high blood pool activity of the $[^{68}\text{Ga}]\text{NODAGA-RGD}$ as a landmark (Fig. 1). The myocardial contours from the $[^{15}\text{O}]\text{water}$ images were copied to the co-registered $[^{68}\text{Ga}]\text{NODAGA-RGD}$ data. Then, the polar maps of $[^{68}\text{Ga}]\text{NODAGA-RGD}$ uptake expressed as standardized uptake value (SUV) (time frame 52–62 min after injection) in the LV myocardium were generated using matching image orientation and sampling points. The region of interest (ROI) defining the ischemic area was copied from the $[^{15}\text{O}]\text{water}$ polar maps to measure $[^{68}\text{Ga}]\text{NODAGA-RGD}$ uptake in this region. The septum was excluded from the measurements to prevent spillover from the blood in the right ventricle. The mean and maximum SUVs were determined from the ischemic area. In order to measure the SUVs, ROI was modified to include only the mid-myocardium in order to avoid spill-over from blood. The maximum SUV within the ROI was determined from area showing visually the highest uptake. One segment in the posterolateral wall (segment 11) that was always outside the ischemic area was used to measure $[^{68}\text{Ga}]\text{NODAGA-RGD}$ uptake in the remote myocardium. The ischemic-to-remote SUV ratio was calculated in the ischemic area and remote myocardium.

Blood sampling and analyses

During the $[^{68}\text{Ga}]\text{NODAGA-RGD}$ PET imaging, blood samples (2 ml) were obtained into heparinized tubes from the femoral artery 2, 5, 10, 20, 30, 40, 50 and 60 min after the injection of $[^{68}\text{Ga}]\text{NODAGA-RGD}$ for the measurements of total radioactivity, radiometabolites

(proportion of authentic tracer), and plasma-to-blood ratio. The radioactivities of whole blood and blood plasma were measured using a gamma counter (1480 Wizard 3[™]; PerkinElmer, Turku, Finland).

Tissue sampling, autoradiography and histology

Immediately after the PET scanning, the animals were sacrificed by an i.v. injection of potassium chloride (B. Braun Medical Oy, Helsinki, Finland). The heart was excised, the LV was cut into 4 short axis slices from base to apex that were incubated for 15 min in 1% TTC (Sigma-Aldrich, Saint Louis, MO, USA), diluted in phosphate-buffered saline (pH 7.4) at 37 °C, photographed from both sides and the presence of non-viable ischemic area was confirmed visually. Based on the TTC staining, transmural samples containing non-viable and immediately adjacent viable myocardium were collected from the LV wall corresponding to the ischemic area in PET images. Another sample was obtained from the posterior LV wall representative of the remote region (segment number 11).

Myocardial samples and a blood sample were weighed and measured for radioactivity using the gamma counter (Wizard). The radioactivity concentration was expressed as standardized uptake values ($\text{SUV} = ([\text{tissue radioactivity}/\text{tissue weight}]/[\text{total given radioactivity}/\text{animal body weight}])$).

Tissue samples were frozen in isopentane mixed with dry ice and cut into serial 40 and 7 μm sections for autoradiography and immunohistochemical stainings respectively, using a cryomicrotome. Tissue sections of 40 μm

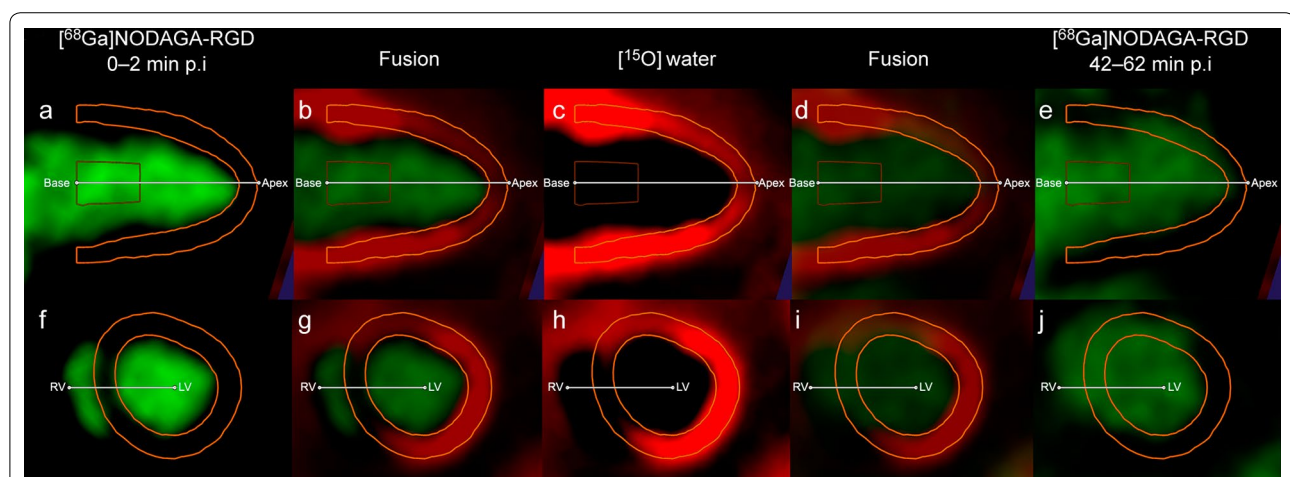


Fig. 1 Co-registration of $[^{68}\text{Ga}]\text{NODAGA-RGD}$ and $[^{15}\text{O}]\text{water}$ PET images and definition of myocardial contours. **a** and **f** demonstrate $[^{68}\text{Ga}]\text{NODAGA-RGD}$ images during the first 2 min after injection of the tracer, **b** and **g** demonstrate the fusion of $[^{15}\text{O}]\text{water}$ PET images (**c**, **h**) and $[^{68}\text{Ga}]\text{NODAGA-RGD}$ images used in the co-registration (**a**, **f**). Yellow lines represent myocardial contours defined in $[^{15}\text{O}]\text{water}$ PET images and copied to the $[^{68}\text{Ga}]\text{NODAGA-RGD}$ images. **d** and **i** demonstrate the fusion of the $[^{15}\text{O}]\text{water}$ PET images (**c**, **h**) and $[^{68}\text{Ga}]\text{NODAGA-RGD}$ images during the last 20 min of the imaging session (**e**, **j**) that demonstrate higher activity in the ischemic area in the anteroseptal wall as compared with the remote myocardium in the inferoposterior wall

thickness were immediately exposed on a phosphor imaging plate (BAS-TR2025, Fuji Photo Film Co. Ltd., Tokyo, Japan) for 2 h. The distribution of radioactivity on the plate was visualized and quantified using a Fluorescent Image Analyzer (Fujifilm FLA-5100, Fuji Photo Film Co. Ltd., Tokyo, Japan). Autoradiographs and hematoxylin & eosin (HE) staining images of the same sections were co-registered and [^{68}Ga]NODAGA-RGD accumulation was measured by drawing ROIs covering remote myocardium, and either viable or injured ischemic myocardium using TINATM 2.10f software (Raytest Isotopenmessgeräte GmbH, Straubenhardt, Germany). Results were expressed as photostimulated luminescence per square millimetre (PSL/mm²) and normalized for the injected radioactivity dose, animal weight and the radioactivity decay.

Serial tissue sections of 7 μm were stained with H&E for general histology, Masson's trichrome for differentiation myocytes and collagenous scar, and immunohistochemistry with antibodies against of CD31 on endothelial cells (dilution 1:250, Thermo Scientific, Cheshire, UK), $\alpha_v\beta_3$ integrin (dilution 1:200, Millipore, Temecula, CA, USA) and α -smooth muscle actin on myofibroblasts (dilution 1:30,000, Sigma-Aldrich, St. Louis, MO, USA). Envision (Dako, Glostrup, Denmark) and Vectastain ABC (Vector Laboratories, Burlingame, CA, USA) kits were used for detection, respectively.

Statistical analyses

All data are expressed as mean \pm SD. Statistical analysis was done with SPSS Statistics software v. 21 (IBM, NY, USA). A paired Student's t test was applied for comparisons of the values between ischemic and remote areas. Comparisons of viable ischemic, injured ischemic and remote areas were done using ANOVA with Dunnett's correction for remote group. A Pearson's rank test (r) was used to analyze correlation between autoradiography and

$\alpha_v\beta_3$ integrin immunohistochemistry. p values less than 0.05 were considered statistically significant.

Results

All the pigs survived the follow-up period. As shown in Fig. 2, perfusion imaging with [^{15}O]water PET during adenosine stress showed a regional perfusion defect corresponding to the ischemic myocardium subtended by the stented LAD in 8 pigs that formed the final study group.

Myocardial blood flow

The average size of the ischemic area defined as MBF < 80% of the maximum during adenosine stress was $30 \pm 10\%$ of the LV as shown in Table 1. There was a regional reduction in resting perfusion within the ischemic area in 2 pigs showing reversible abnormality in the border areas. The average MBF in the ischemic area was lower than in the remote myocardium both at rest (1.4 ± 0.46 vs. 1.6 ± 0.41 ml/g/min, $p = 0.0026$) and during adenosine stress (1.9 ± 1.1 vs. 4.0 ± 2.2 ml/g/min, $p = 0.0036$). The average rate pressure product at rest and during adenosine stress was $14,000 \pm 4500$ and $14,000 \pm 3700$ mmHg bpm, respectively.

Histology

In 6 pigs TTC staining showed partially injured myocardium within the ischemic area. In 4 pigs there was subendocardial injury within 1 or 2 segments, and in 2 pigs there was partially transmural injury extending to 3 segments.

Histological findings in tissue samples from the remote area and viable ischemic or injured area are described in Figs. 3 and 4. Tissue sections from the injured area showed characteristic histological features of recent ischemic myocardial injury. There was mainly loose connective tissue with some mature collagen fibers among

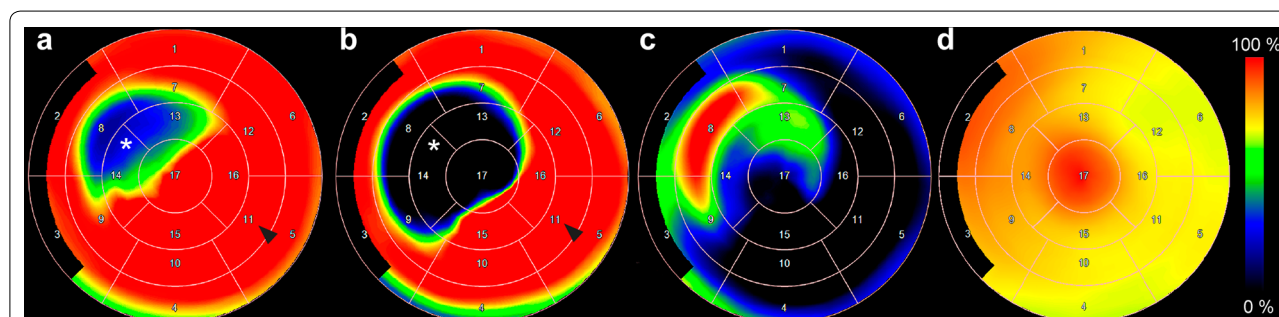


Fig. 2 Cardiac [^{68}Ga]NODAGA-RGD and [^{15}O]water in vivo PET analyses. **a** and **b** demonstrate polar maps of MBF measured by [^{15}O]water PET at rest and during adenosine stress, respectively. **c** and **d** show polar maps of [^{68}Ga]NODAGA-RGD uptake. Note the presence of increased [^{68}Ga]NODAGA-RGD uptake in **c** co-localizing with an area of reduced myocardial perfusion (asterisk in **a, b**) as compared with the remote area (arrowhead in **a, b**). Distribution of [^{68}Ga]NODAGA-RGD is homogenous in the left ventricle of sham operated pig (**d**)

Table 1 Cardiac [¹⁵O]water and [⁶⁸Ga]NODAGA-RGD PET

Animal	[¹⁵ O]water PET	[⁶⁸ Ga]NODAGA-RGD PET		
	Ischemic area (% of the LV)	Remote SUV _{Mean}	Ischemic area SUV _{Mean}	Injured area SUV _{Max}
1	19	0.68	0.71	0.95
2	17	0.37	0.56	0.67
3	35	0.52	0.70	1.11
4	32	0.47	0.56	0.74
5	19	0.36	0.54	0.72
6	36	0.65	0.79	0.94
7	37	0.42	0.41	0.59
8	43	0.45	0.57	0.70
Mean	30	0.49	0.61*	0.80 [†]
SD	10	0.12	0.12	0.18

The size of ischemic area based on [¹⁵O]water PET during adenosine stress and myocardial [⁶⁸Ga]NODAGA-RGD uptake shown as standardized uptake value (SUV) in the remote myocardium, in the ischemic area and at the site of the highest uptake (Max) within the ischemic area

SUV standardized uptake value, LV left ventricle

* $p = 0.0034$ vs. remote

[†] $p < 0.001$ vs. remote

a large amount of myofibroblasts and inflammatory cells. Viable ischemic areas showed normal distribution of myocytes and connective tissue, but some myocyte vacuolization probably related to ischemia was seen. The remote myocardium appeared histologically normal.

The immunohistochemical staining of CD31 showed positive staining in endothelial cells lining the capillaries (Fig. 3). There was no statistically significant difference in the areal percentage of the myocardium stained with CD31 between the remote myocardium and either the viable ischemic or the injured myocardium (Fig. 4).

The immunohistochemical staining of $\alpha_v\beta_3$ integrin was localized around the capillaries in the viable myocardium, but also showed a diffuse distribution in the injured myocardium (Fig. 3). The areal percentage of the

myocardium stained with $\alpha_v\beta_3$ integrin was higher in the injured area than in the remote myocardium ($23 \pm 1.9\%$ vs. $7.5 \pm 1.0\%$, $p < 0.001$), but there was no difference between the viable ischemic myocardium ($10 \pm 4.0\%$ vs. $7.5 \pm 1.0\%$, $p = 0.15$) and the remote area (Fig. 4).

There was intense α -SMA positive staining in the injured myocardium (Fig. 3). The area of the myocardium stained with α -SMA antibody was higher in the injured than in the remote area ($7.2 \pm 2.9\%$ vs. $1.3 \pm 0.75\%$, $p = 0.019$).

Radiochemical analyses and protein binding

The radiochemical purity and specific radioactivity of [⁶⁸Ga]NODAGA-RGD were >99% and 35 ± 2.8 GBq/ μ mol at the end of syntheses, respectively. The tracer

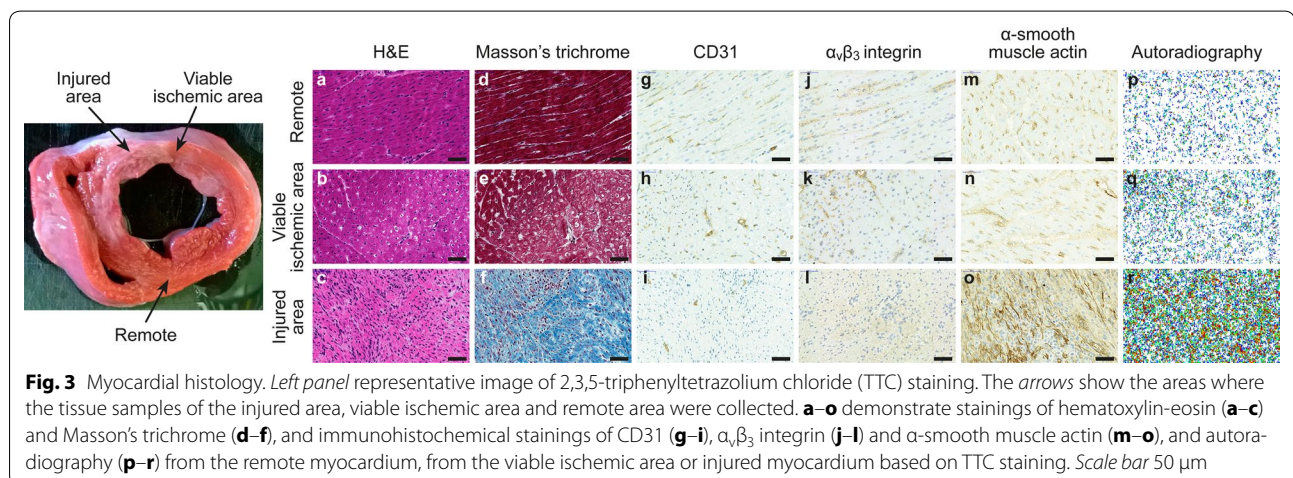
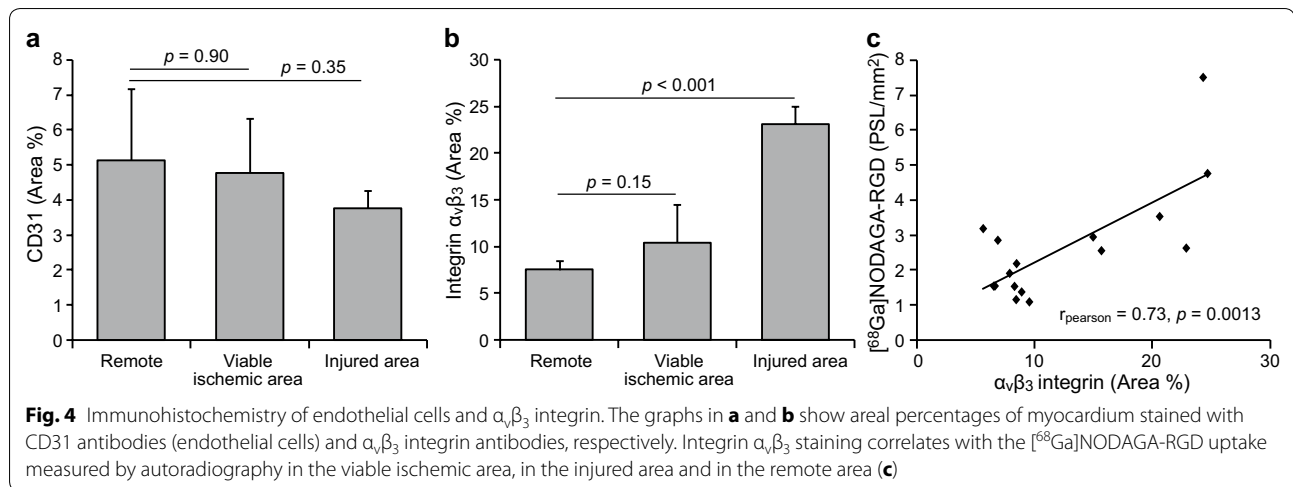


Fig. 3 Myocardial histology. *Left panel* representative image of 2,3,5-triphenyltetrazolium chloride (TTC) staining. The *arrows* show the areas where the tissue samples of the injured area, viable ischemic area and remote area were collected. **a–o** demonstrate stainings of hematoxylin-eosin (**a–c**) and Masson's trichrome (**d–f**), and immunohistochemical stainings of CD31 (**g–i**), $\alpha_v\beta_3$ integrin (**j–l**) and α -smooth muscle actin (**m–o**), and autoradiography (**p–r**) from the remote myocardium, from the viable ischemic area or injured myocardium based on TTC staining. Scale bar 50 μ m



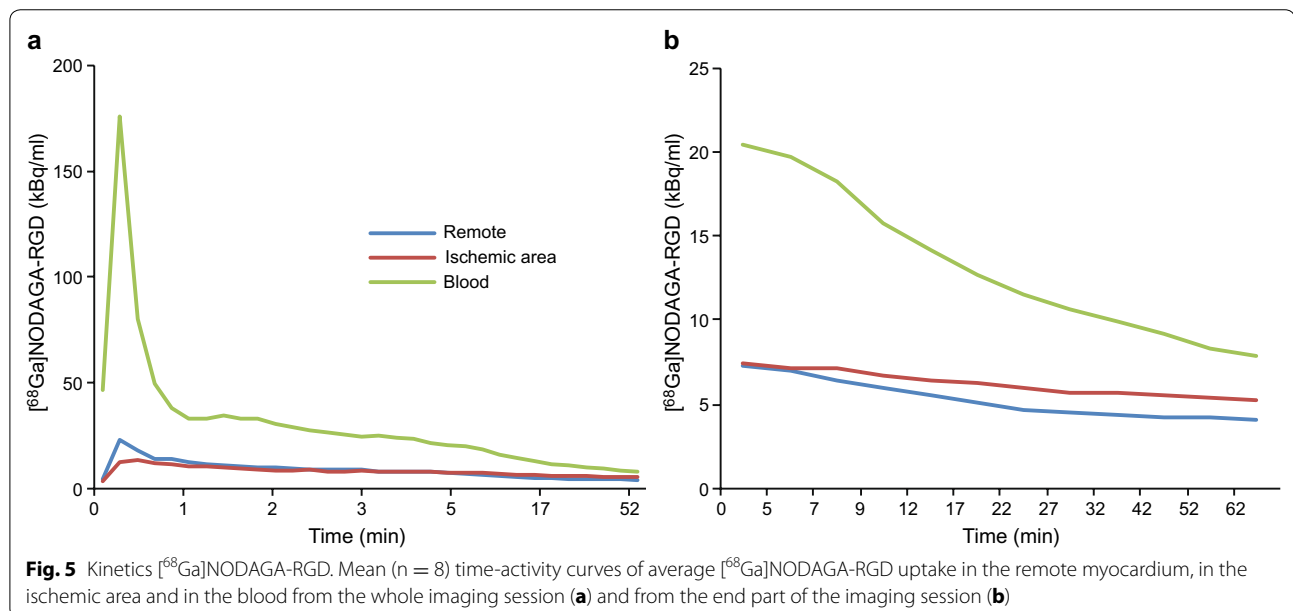
remained stable in vivo throughout the PET imaging with the proportion of intact tracer being >98%. The plasma-to-blood ratio of the tracer was 1.4 ± 0.10 . The plasma free fraction was 0.94 ± 0.011 in the rat, 0.93 ± 0.017 in the pig and 0.91 ± 0.081 in the human serum. Thus, binding of the tracer in the plasma proteins was low in all tested species.

^{68}Ga]NODAGA-RGD PET Imaging

Analysis of the ^{68}Ga]NODAGA-RGD PET images is demonstrated in Figs. 1 and 2, and time-activity curves are shown in Fig. 5. There was virtually no tracer uptake in the normal LV myocardium and tracer activity in the blood pool remained higher than myocardial

activity throughout the imaging. Based on the ^{15}O] water PET images, myocardial contours were drawn in the ^{68}Ga]NODAGA-RGD images to analyze regional tracer uptake. This demonstrated homogenous ^{68}Ga]NODAGA-RGD distribution in sham operated pigs (coefficient of variation between segments $15 \pm 6.3\%$), whereas uptake was regionally increased in all stented pigs within the ischemic area defined from the ^{15}O] water perfusion imaging.

Mean and maximum myocardial ^{68}Ga]NODAGA-RGD uptakes in the ischemic area and in the remote myocardium of stented pigs are shown in Table 1 and Fig. 6. In the ischemic area, the average myocardial ^{68}Ga]NODAGA-RGD uptake was 26% higher than in the



remote myocardium ($p = 0.003$). The maximum uptake values inside the ischemic area of the pigs were 73 and 46% higher than in the remote myocardium in pigs with viable ischemic or injured myocardium, respectively ($p = 0.010$ and $p = 0.013$, respectively, Table 1). There was no correlation between the size of the ischemic area and the amount of [^{68}Ga]NODAGA-RGD uptake. The average [^{68}Ga]NODAGA-RGD uptake in the LV myocardium of the sham group was similar to the remote area of the stented pigs (SUV 0.42 ± 0.10 vs. 0.49 ± 0.12 ($p = 0.38$) and there was no difference in the uptake between the anteroseptal (segments 7 and 13) and posterolateral (segment 11) walls in the sham group (SUV 0.39 ± 0.11 vs. 0.36 ± 0.078 , $p = 0.28$).

[^{68}Ga]NODAGA-RGD ex vivo biodistribution

Ex vivo biodistribution studies (Fig. 6) showed that the radioactivity from [^{68}Ga]NODAGA-RGD was higher in the tissue sample obtained from the injured myocardium (TTC negative) compared to the tissue sample obtained from the remote myocardium (SUV 0.79 ± 0.21 vs. 0.49 ± 0.21 , $p = 0.016$), but there was no difference between the samples obtained from the remote myocardium and the viable ischemic (TTC positive) myocardium (SUV 0.49 ± 0.17 , $p = 0.99$).

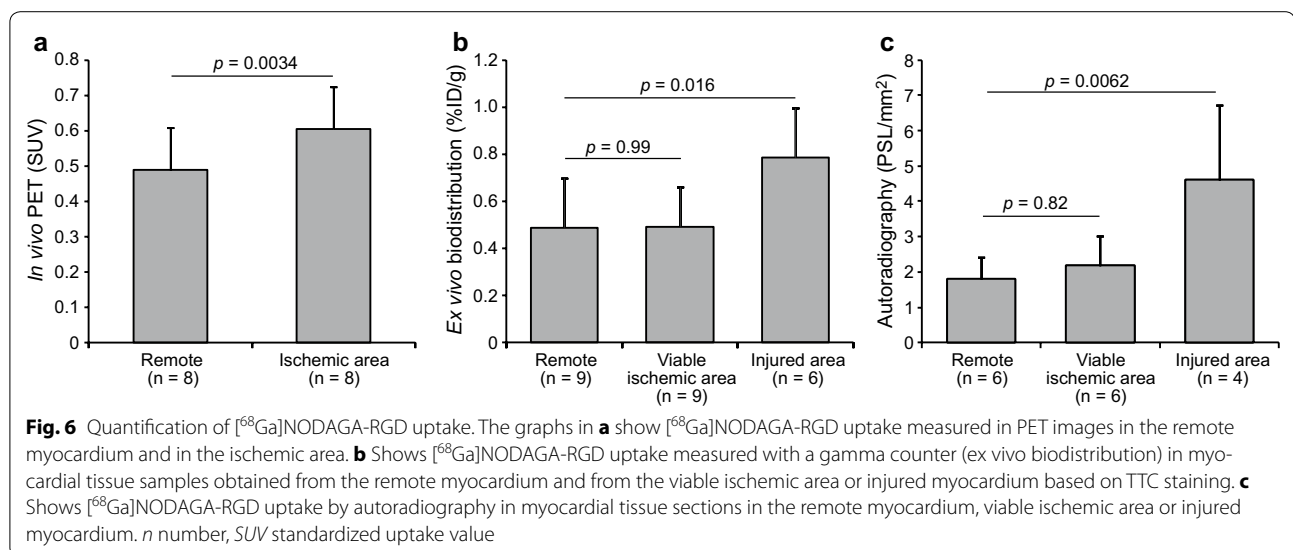
[^{68}Ga]NODAGA-RGD autoradiography

An autoradiography was performed on 6 pigs. The autoradiographs (Fig. 3) showed no [^{68}Ga]NODAGA-RGD uptake in tissue sections from the remote myocardium. Uptake was also very low in the viable ischemic myocardium adjacent to the injured myocardium. In contrast, there were areas with clearly increased uptake in the

sections containing injured myocardium. Quantitatively (Fig. 6), there was a statistically significant difference in the uptake between injured and remote myocardium ($p = 0.006$), whereas there was no difference in the uptake between viable ischemic myocardium and in the remote area ($p = 0.82$). The mean uptake values in the viable ischemic, remote, and injured areas were 2.2 ± 0.85 , 1.8 ± 0.61 and 4.6 ± 2.1 PSL/ mm^2 , respectively. The [^{68}Ga]NODAGA-RGD uptake measured by autoradiography positively correlated to the area percentage of $\alpha_v\beta_3$ integrin staining in the tissue sections ($r_{\text{Pearson}} = 0.73$, $p = 0.0013$) (Fig. 4).

Discussion

The main findings of the present study are that [^{68}Ga]NODAGA-RGD cardiac PET detected increased myocardial $\alpha_v\beta_3$ integrin expression two weeks after induction of flow-limiting coronary stenosis in pig. In this model, $\alpha_v\beta_3$ integrin expression and [^{68}Ga]NODAGA-RGD uptake localized to the irreversibly injured myocardium, whereas tracer uptake was absent in viable ischemic areas. These results indicate that [^{68}Ga]NODAGA-RGD is a potentially sensitive tool to detect areas of recent myocardial injury in the presence of chronic ischemia. These findings have implications in evaluation of patients with chronic ischemic heart disease in whom a mixture of viable ischemic and injured myocardium exists in the absence of transmural scar [23]. Expression of $\alpha_v\beta_3$ integrin appears to play a central role in cardiac repair following myocardial infarction. A recent study showed in patients with acute myocardial infarction that $\alpha_v\beta_3$ integrin targeted tracer ^{18}F -fluciclatide uptake was highest in segments with improved contractile function [24]. Thus,



imaging of $\alpha_v\beta_3$ integrin expression may have potential to predict functional recovery upon reperfusion [24, 25] or monitor effects of therapies aimed at accelerating repair of myocardial injury.

[^{68}Ga]NODAGA-RGD is a novel PET tracer for imaging $\alpha_v\beta_3$ integrin expression composed of a pentacyclic peptide binding moiety Arg-Gly-Asp-D-Tyr-Lys coupled with the gallium chelating agent NODAGA. The precursor can be obtained in Good Manufacturing Practices quality from a commercial supplier and the tracer is being developed for clinical use [26]. In addition to good target specificity, studies have indicated favorable kinetics, dosimetry and safety profile [27, 28]. In previous studies, [^{68}Ga]NODAGA-RGD uptake demonstrated $\alpha_v\beta_3$ integrin expression in infarcted rat myocardium 1 week after coronary ligation [5]. Our study adds to the previous work by demonstrating that [^{68}Ga]NODAGA-RGD cardiac PET detected $\alpha_v\beta_3$ integrin expression in small, mainly subendocardial areas of myocardial injury in a model of chronic ischemia. We used a bottleneck stent model to induce persistent flow-limiting stenosis in pigs. Pig offers several advantages in comparison to rodent models as a model of translational cardiovascular research. The heart and the coronary artery system of pigs are almost identical to those of humans [29]. The size of the pig heart, which is more comparable to the size of the human heart than the heart of rodents, enables the use of clinical scanner and more reliable discrimination between the injured and ischemic myocardial areas. As shown earlier in this model, stent implantation immediately causes severe reduction in blood flow in the target coronary artery as shown by reduced fractional flow reserve, reduced myocardial blood flow during adenosine stress, and rapid collateral growth [19]. Although antithrombotic therapy was continued throughout the study to prevent stent occlusion, areas of organizing injury were detected in 6 animals. This may have been caused by insufficient compensation for reduction in myocardial perfusion by collateral formation, occlusion of a side branch by the stent, or thrombosis within the stent [19].

Repair following myocardial injury is triggered by a complex interaction of neurohormonal activation and upregulation of local paracrine signaling mechanisms that initiate restoration of capillary network through angiogenesis and extracellular matrix remodeling through macrophage accumulation and fibroblast activation. Expression of $\alpha_v\beta_3$ integrin by vascular endothelial cells mediates angiogenesis, but also plays a role in regulation of macrophage inflammatory responses and myofibroblast differentiation during this process [16–18]. Thus, $\alpha_v\beta_3$ integrin is a potential marker of repair following myocardial infarction. One main finding of our study

is that [^{68}Ga]NODAGA-RGD uptake was localized in the irreversibly damaged myocardial regions, but not in the adjacent viable myocardium within the ischemic area in this model. Increased expression of $\alpha_v\beta_3$ integrin was confirmed by immunohistochemical staining, the amount of which correlated with [^{68}Ga]NODAGA-RGD uptake in myocardial tissue samples. In the injured myocardium, staining of $\alpha_v\beta_3$ integrin was diffuse among fibroblasts and inflammatory cells, and staining of α -SMA demonstrated myofibroblast differentiation, whereas endothelial cell staining with CD31 antibody demonstrated no difference in capillary density between remote, ischemic, and infarcted myocardium. These findings indicate that $\alpha_v\beta_3$ integrin expression and [^{68}Ga]NODAGA-RGD uptake reflected not only angiogenesis, but other processes related to scar formation. These findings are in line with a previous study that did not find evidence of enhanced angiogenesis or uptake of ^{123}I -labelled cyclo(-Arg-Gly-Asp-D-Tyr-Lys(3-acetamido-2,6-anhydro-3-deoxy- β -D-glycero-D-gulo-heptanoic acid) (Gluc-RGD) in a pig model of myocardial hibernation induced by an ameroid constrictor [30]. Previous studies have shown RGD uptake and angiogenesis in severely hypoxic tissue [9, 12], but the severity and duration of the ischemia in the viable ischemic myocardium in our model were probably not sufficient to induce these.

We acknowledge that there are some limitations associated with our study. One of these is the fact that we did not test the effects of therapeutic angiogenesis on [^{68}Ga]NODAGA-RGD uptake. Angiogenesis induced with gene therapy has previously been detected with [^{123}I]-Gluc-RGD in hibernating pig myocardium, where spontaneous ischemia did not induce angiogenesis [30] and with [^{18}F]-alfatide II ([^{18}F]-AIF-NOTA-E[PEG₄-c(RGDfk)]₂) in rats after myocardial infarction [31]. Another limitation is that we used only one time point based on previous studies showing a peak in $\alpha_v\beta_3$ integrin expression and RGD uptake between 1 and 4 weeks after an ischemic insult [3, 4, 6, 16]. We also acknowledge the small sample size in our study, especially relating to the autoradiography. Also the use of two different PET/CT scanners for [^{15}O]water and [^{68}Ga]NODAGA-RGD imaging due to logistic reasons is a limitation and might affect the accuracy of the co-registration of the images. Adenosine dose was adjusted in some pigs due to variable systemic hemodynamic responses. It has been shown that dipyridamole may provide stronger hyperemic response in the pig heart [32]. Respiratory and cardiac motion may affect sensitivity of [^{68}Ga]NODAGA-RGD due to activity in the closely associated blood pool. Myocardial [^{68}Ga]NODAGA-RGD uptake was studied at 50–60 min after injection, when blood levels were lower than 5% of their peak. Consistent

with previous studies [24], [⁶⁸Ga]NODAGA-RGD radioactivity remained higher in the blood than in the normal myocardium. In order to avoid spill over from the right ventricle influencing our results we included only segments in the mid-anterolateral and posterior wall into the in vivo PET analysis. Integrin $\alpha_v\beta_3$ can be found on platelets, albeit in low concentrations [33]. Platelet count in pigs is much higher than that of humans [34] that might result in higher blood radioactivity in pigs than in human. However, we did not find any species differences in the binding of the tracer to plasma proteins between pigs, rats and humans.

Conclusions

[⁶⁸Ga]NODAGA-RGD cardiac PET demonstrates increased myocardial $\alpha_v\beta_3$ integrin expression in a pig model of coronary stenosis. Increased $\alpha_v\beta_3$ integrin expression is localized in the irreversibly injured myocardium, whereas it is absent in viable myocardium within the ischemic area. [⁶⁸Ga]NODAGA-RGD PET may be useful for the identification of $\alpha_v\beta_3$ integrin activation associated with repair of myocardial injury in the presence of coronary stenosis.

Abbreviations

RGD: arginyl-glycyl-aspartic acid; ECM: extracellular matrix; PET: positron emission tomography; NODAGA: 1,4,7-triazacyclononane-1-glutaric acid-4,7-diacetic acid; LAD: left anterior descending coronary artery; TTC: 2,3,5-triphenyltetrazolium chloride; RP-HPLC: high-performance liquid chromatography; TFA: trifluoroacetic acid; TAC: time-activity curve; VOI: volume of interest; LV: left ventricle; MBF: myocardial blood flow; SUV: standardized uptake value; ROI: region of interest; HE: hematoxylin & eosin; PSL: photostimulated luminescence; Gluco-RGD: cyclo(-Arg-Gly-Asp-D-Tyr-Lys(3-acetamido-2,6-anhydro-3-deoxy- β -D-glycero-D-gulo-heptanoic acid).

Authors' contributions

Planning: MG, MT, TS, SY-H, JK, AR and AS; conducting: MG, MT, TK, PH, AK, TS, TT, JT, MK, OM, MP, PS, SY-H, JK, AR and AS; reporting: MG, MT, TK, PH, AK, TS, TT, JT, MK, OM, MP, PS, SY-H, JK, AR and AS. All authors read and approved the final manuscript.

Author details

¹ Turku PET Centre, University of Turku, 20521 Turku, Finland. ² Heart Center, Turku University Hospital, Turku, Finland. ³ A.I.Virtanen Institute for Molecular Sciences, University of Eastern Finland, Joensuu, Finland. ⁴ Research Centre of Applied and Preventive Cardiovascular Medicine, University of Turku, Turku, Finland. ⁵ Turku PET Centre, Turku University Hospital, Turku, Finland. ⁶ Department of Medical Physics, Turku University Hospital and University of Turku, Turku, Finland. ⁷ Department of Forensic Medicine, University of Turku, Turku, Finland. ⁸ Turku Center for Disease Modeling, University of Turku, Turku, Finland. ⁹ Institute of Clinical Medicine, University of Turku, Turku, Finland.

Acknowledgements

The authors thank the staff of the Turku PET Centre for performing PET imaging and laboratory measurements. The authors would also like to thank Mrs Liisa Lempiäinen and Ms Erica Nyman for the preparation of histological samples.

Competing interests

The authors declare that they have no competing interests.

Availability of data and materials

The datasets used and/or analysed during the current study are available from the corresponding author on reasonable request.

Ethics approval and consent to participate

All animal experiments were approved by the Lab-Animal Care & Use Committee of the State Provincial Office of Southern Finland and carried out in compliance with the EU legislation relating to the conduct of animal experimentation.

Funding

The study was funded by Tekes—the Finnish Funding Agency for Technology and Innovation, the Finnish Foundation for Cardiovascular Research and Sigrid Juselius Foundation. The study was conducted in the Finnish Centre of Excellence in Cardiovascular and Metabolic Disease supported by the Academy of Finland, University of Turku, Turku University Hospital, and Åbo Akademi University. M.G. is a PhD student supported by the Drug Research Doctoral Programme, University of Turku Graduate School, Turku, Finland.

Publisher's Note

Springer Nature remains neutral with regard to jurisdictional claims in published maps and institutional affiliations.

Received: 9 March 2017 Accepted: 15 June 2017

Published online: 19 June 2017

References

- Brooks PC, Clark RA, Cheresh DA. Requirement of vascular integrin alpha v beta 3 for angiogenesis. *Science*. 1994;264:569–71.
- Manso AM, Kang S-M, Ross RS. Integrins, focal adhesions, and cardiac fibroblasts. *J Investig Med*. 2009;57:856–60.
- Meoli DF, Sadeghi MM, Krassilnikova S, Bourke BN, Giordano FJ, Dione DP, et al. Noninvasive imaging of myocardial angiogenesis following experimental myocardial infarction. *J Clin Invest*. 2004;113:1684–91.
- Higuchi T, Bengel FM, Seidl S, Watzlowik P, Kessler H, Hegenloh R, et al. Assessment of $\alpha_v\beta_3$ integrin expression after myocardial infarction by positron emission tomography. *Cardiovasc Res*. 2008;78:395–403.
- Laitinen I, Notni J, Pohle K, Rudelius M, Farrell E, Nekolla SG, et al. Comparison of cyclic RGD peptides for $\alpha_v\beta_3$ integrin detection in a rat model of myocardial infarction. *EJNMMI Res*. 2013;3:38.
- Kiugel M, Dijkgraaf I, Kytö V, Helin S, Liljenbäck H, Saanijoki T, et al. Dimeric [(68)Ga]DOTA-RGD peptide targeting $\alpha_v\beta_3$ integrin reveals extracellular matrix alterations after myocardial infarction. *Mol Imaging Biol*. 2014;16:793–801.
- Menichetti L, Kusmic C, Panetta D, Arosio D, Petroni D, Matteucci M, et al. MicroPET/CT imaging of $\alpha_v\beta_3$ integrin via a novel ⁶⁸Ga-NOTA-RGD peptidomimetic conjugate in rat myocardial infarction. *Eur J Nucl Med Mol Imaging*. 2013;40:1265–74.
- Gao H, Lang L, Guo N, Cao F, Quan Q, Hu S, et al. PET imaging of angiogenesis after myocardial infarction/reperfusion using a one-step labeled integrin-targeted tracer 18F-AIF-NOTA-PRGD2. *Eur J Nucl Med Mol Imaging*. 2012;39:683–92.
- Kalinowski L, Dobrucki LW, Meoli DF, Dione DP, Sadeghi MM, Madri JA, et al. Targeted imaging of hypoxia-induced integrin activation in myocardium early after infarction. *J Appl Physiol*. 2008;104:1504–12.
- van den Borne SWM, Isobe S, Verjans JW, Petrov A, Lovhag D, Li P, et al. Molecular imaging of interstitial alterations in remodeling myocardium after myocardial infarction. *J Am Coll Cardiol*. 2008;52:2017–28.
- Dobrucki LW, Tsutsumi Y, Kalinowski L, Dean J, Gavin M, Sen S, et al. Analysis of angiogenesis induced by local IGF-1 expression after myocardial infarction using microSPECT-CT imaging. *J Mol Cell Cardiol*. 2010;48:1071–9.
- Dobrucki LW, Meoli DF, Hu J, Sadeghi MM, Sinusas AJ. Regional hypoxia correlates with the uptake of a radiolabeled targeted marker of angiogenesis in rat model of myocardial hypertrophy and ischemic injury. *J Physiol Pharmacol*. 2009;60(Suppl 4):117–23.

13. Sherif HM, Saraste A, Nekolla SG, Weidl E, Reder S, Tapfer A, et al. Molecular imaging of early $\alpha v\beta 3$ integrin expression predicts long-term left-ventricle remodeling after myocardial infarction in rats. *J Nucl Med*. 2012;53:318–23.
14. Sun Y, Zeng Y, Zhu Y, Feng F, Xu W, Wu C, et al. Application of (68)Ga-PRGD2 PET/CT for $\alpha v\beta 3$ -integrin imaging of myocardial infarction and stroke. *Theranostics*. 2014;4:778–86.
15. Rasmussen T, Follin B, Kastrup J, Brandt-Larsen M, Madsen J, Emil Christensen T, et al. Angiogenesis PET tracer uptake (68 Ga-NODAGA-E[(cRGDyK)]2) in induced myocardial infarction in minipigs. *Diagnostics*. 2016;6:26.
16. Sun M, Opavsky MA, Stewart DJ, Rabinovitch M, Dawood F, Wen WH, et al. Temporal response and localization of integrins $\beta 1$ and $\beta 3$ in the heart after myocardial infarction: regulation by cytokines. *Circulation*. 2003;107:1046–52.
17. Antonov AS, Antonova GN, Munn DH, Mivechi N, Lucas R, Cattravas JD, et al. $\alpha v\beta 3$ integrin regulates macrophage inflammatory responses via PI3 kinase/Akt-dependent NF- κB activation. *J Cell Physiol*. 2011;226:469–76.
18. Sarrazy V, Koehler A, Chow ML, Zimina E, Li CX, Kato H, et al. Integrins $\alpha v\beta 5$ and $\alpha v\beta 3$ promote latent TGF- $\beta 1$ activation by human cardiac fibroblast contraction. *Cardiovasc Res*. 2014;102:407–17.
19. Rissanen TT, Nurro J, Halonen PJ, Tarkia M, Saraste A, Rannankari M, et al. The bottleneck stent model for chronic myocardial ischemia and heart failure in pigs. *Am J Physiol Heart Circ Physiol*. 2013;305:H1297–308.
20. Tarkia M, Saraste A, Saanjoki T, Oikonen V, Vähäsilta T, Strandberg M, et al. Evaluation of 68 Ga-labeled tracers for PET imaging of myocardial perfusion in pigs. *Nucl Med Biol*. 2012;39:715–23.
21. Tarkia M, Stark C, Haavisto M, Kentala R, Vähäsilta T, Savunen T, et al. Cardiac remodeling in a new pig model of chronic heart failure: Assessment of left ventricular functional, metabolic, and structural changes using PET, CT, and echocardiography. *J Nucl Cardiol*. 2015;22:655–65.
22. Kajander SA, Joutsiniemi E, Saraste M, Pietilä M, Ukkonen H, Saraste A, et al. Clinical value of absolute quantification of myocardial perfusion with (15)O-water in coronary artery disease. *Circ Cardiovasc Imaging*. 2011;4:678–84.
23. Elsasser A, Schlepper M, Klovekorn W-P, Cai W-J, Zimmermann R, Müller K-D, et al. Hibernating myocardium: an incomplete adaptation to ischemia. *Circulation*. 1997;96:2920–31.
24. Jenkins WS, Vesey AT, Stirrat C, Connell M, Lucatelli C, Neale A, et al. Cardiac $\alpha v\beta 3$ integrin expression following acute myocardial infarction in humans. *Heart*. 2017;103:607–15.
25. Windecker S, Kolh P, Alfonso F, Collet J-P, Cremer J, Falk V, et al. ESC/EACTS guidelines on myocardial revascularization. *Eur Heart J*. 2014;35:2541–619.
26. Van Der Gucht A, Pomoni A, Jreige M, Allemann P, Prior JO. 68Ga-NODAGA-RGDyK PET/CT imaging in esophageal cancer: First-in-Human Imaging. *Clin Nucl Med* 2016;41:e491–2.
27. Buchegger F, Viertl D, Baechler S, Dunet V, Kosinski M, Poitry-Yamate C, et al. 68Ga-NODAGA-RGDyK for $\alpha v\beta 3$ integrin PET imaging. *Nuklearmedizin*. 2011;50:225–33.
28. Knetsch PA, Petrik M, Griessinger CM, Rangger C, Fani M, Kesenheimer C, et al. [68Ga]NODAGA-RGD for imaging $\alpha v\beta 3$ integrin expression. *Eur J Nucl Med Mol Imaging*. 2011;38:1303–12.
29. Swindle MM, Makin A, Herron AJ, Clubb FJ, Frazier KS. Swine as models in biomedical research and toxicology testing. *Vet Pathol*. 2012;49:344–56.
30. Johnson LL, Schofield L, Donahay T, Bouchard M, Poppas A, Haubner R. Radiolabeled arginine-glycine-aspartic acid peptides to image angiogenesis in swine model of hibernating myocardium. *JACC Cardiovasc Imaging*. 2008;1:500–10.
31. Cai M, Ren L, Yin X, Guo Z, Li Y, He T, et al. PET monitoring angiogenesis of infarcted myocardium after treatment with vascular endothelial growth factor and bone marrow mesenchymal stem cells. *Amino Acids*. 2016;48:811–20.
32. Rasmussen T, Follin B, Kastrup J, Christensen TE, Hammelev KP, Kjær A, et al. Myocardial perfusion of infarcted and normal myocardium in propofol-anesthetized minipigs using 82Rubidium PET. *J Nucl Cardiol*. 2016;23:599–603.
33. Bennett JS, Berger BW, Billings PC. The structure and function of platelet integrins. *J Thromb Haemost*. 2009;7(Suppl 1):200–5.
34. Chen Y, Qin S, Ding Y, Li S, Yang G, Zhang J, et al. Reference values of biochemical and hematological parameters for Guizhou minipigs. *Exp Biol Med*. 2011;236:477–82.

Submit your next manuscript to BioMed Central and we will help you at every step:

- We accept pre-submission inquiries
- Our selector tool helps you to find the most relevant journal
- We provide round the clock customer support
- Convenient online submission
- Thorough peer review
- Inclusion in PubMed and all major indexing services
- Maximum visibility for your research

Submit your manuscript at
www.biomedcentral.com/submit

